

Experimental Detection of Spur Gear Eccentricity Severity Through Denoised FFT and STFT Analysis

Vhahangwele Colleen Sigonde¹, Desejo Filipeson Sozinando^{1*}, Bernard Xavier Tchomeni kouejou¹ and Alfayo Anyika Alugongo¹

¹Vaal University of Technology, Vanderbijlpark, Department of Industrial Engineering, Operations Management and Mechanical Engineering, South Africa.

Abstract. Eccentricity in spur gears commonly results from manufacturing tolerances and assembly errors, generating periodic geometric deviations that affect gear-mesh dynamics and vibration signatures. An experimental study is undertaken to assess eccentricity severity using denoised Fast Fourier Transform (FFT) and Short-Time Fourier Transform (STFT) analyses. The experimental setup consists of a two-stage spur gearbox test rig fitted with radial accelerometers on the bearing housings of both the input and output shafts. Fault severity was systematically varied by attaching eccentric masses of 200 g, 400 g, and 890 g to the driven gear while maintaining constant operating conditions. Prior to frequency analysis, vibration signals were processed with a causal IIR filter to reduce background noise. FFT results showed a clear amplification of sidebands around the gear-mesh frequency and its harmonics as eccentricity increased. STFT representations further highlighted persistent and evenly spaced time–frequency components aligned with the mesh frequency, particularly at higher eccentricity levels.

1 Introduction

It has been shown that numerous studies have focused on different aspects of gear dynamics. A plenty of investigation works have demonstrated that a significant amount of the vibrational features of the spur gear system depend heavily upon its specific gear eccentricity. Generally, the process of installing and manufacturing gears will bring about discrepancy in the degree of gear eccentricity, which causes changes to time-variant parametric values like contact ratio, the pressure angle and meshing rigidity. These subsequently induce dramatic variations on the dynamical reaction of gear systems. Deviations in paths travelled by gears themselves will occur when there exist differences in the two kinds of parameters aforementioned above and they are much more disparate from what occurs in gears without any degree of eccentricity, thus having great influences on both overall safety/ performances and quantifiable performance criteria for this gear system[1]. Besides, although researchers believe that other extra-dynamical factors which can affect the level of generated sound/vibration could bring about corresponding alteration on levels of sound/vibration in transmission-based gears in terms of profiled deviations in teeth-of-gears and slight misalignment, the presence of eccentricity itself would supposedly enlarge adverse effects brought about by aforementioned factors aforementioned[2][3], thereby producing extremely complicated multistate meshing behaviours experienced by the whole system (including events such as mesh

failure and reverse side) that make it difficult to determine actual dynamic responses presented above[4]; likewise, the occurrence of intrinsic excitations within a system, caused by manifestations of fracture problems or those developed because of experiences generated due to rubbing etc.[6], suffers more exacerbation along with errors of eccentricity involved therein. The internal movements of gear transmissions create noise and vibration. This noise and vibration affect how well gear transmissions work and how precise they are. The way the center of the gear is not perfectly. The movement of the gears interact with each other is important. We need to make models and analyze them to understand and prevent bad vibrations in spur gear systems. Advanced models that look at how the center of the gear's not perfectly aligned and other things like how the space, between the gears changes over time and random loads help us understand the complex behavior of gear transmissions and how stable they are [7]. Artificial Neural Networks are really good at helping us keep an eye on how gearsre doing when they have to work with different loads and speeds. It is needed to use them with methods to look at the vibrations from motors and find problems really accurately. We also use something called Variational Mode Decomposition to break down the vibration signals into parts. Then we look at these parts using statistics. Something called Fast Fourier Transform to see if there are any problems with the gears when they are moving at different speeds. Artificial Neural Networks and Variational Mode Decomposition serve as key techniques in modern gear condition monitoring.

* Corresponding author: desejos@vut.ac.za

Complementary to these methods, complex network theory has been applied by transforming vibration signals into visibility graphs and using the resulting features with error-correcting output codes and support vector machines for multifault diagnosis, demonstrating superior accuracy compared to traditional approaches [10]. Noise-assisted multivariate empirical mode decomposition, when paired with envelope demodulation analysis, has also been employed to capture non-stationary fault information in gear vibration signals [11]. The Maximal Overlap Discrete Wavelet Transform (MODWT) and VMD have been employed to uncover incipient faults by extracting concealed fault signatures from noisy signals, with various classifiers such as Support Vector Machine and Decision Tree employed for classification purposes [12]. Furthermore, an integrated ensemble model that combines Convolutional Neural Networks and Support Vector Machines has been proposed for the diagnosis of both multiple and singular gear faults, leveraging complementary signal processing techniques to augment detection capabilities [13]. Additional innovative methodologies encompass the application of geometric classification techniques to heterogeneous signals, encompassing current, voltage, and vibration data, aimed at diagnosing gear faults under varying operational conditions [14]. Minimum entropy deconvolution and local cepstrum analysis have been utilised in worm gearbox studies to isolate weak fault features, leading to high detection accuracy [15,16]. For spur gears, dimensional analysis combined with support vector machines has been adopted as a fault detection strategy, showing a strong correlation between analytical predictions and experimental data [17]. Finally, several studies report that conventional signal processing techniques may outperform deep learning methods in particular scenarios, emphasising their sustained applicability in gear fault diagnosis [18].

Extensive investigations into gear dynamics and fault diagnosis have been reported. However, experimental detection of gear eccentricity remains non-trivial. The challenge is most significant during early and intermediate fault stages, when vibration responses are weak and frequently masked by noise, background resonances, and interacting meshing effects. A large proportion of recent studies employ complex decomposition techniques or data-driven approaches which, while effective, often obscure the physical mechanisms associated with eccentricity evolution. An experimentally driven framework that explicitly links geometric eccentricity to physically interpretable spectral signatures therefore continues to be of practical and scientific interest. In this context, spur gear eccentricity is investigated using a combined denoised FFT and STFT approach, favouring clarity of physical interpretation over algorithmic complexity. Controlled eccentric masses are introduced to emulate progressive fault severity and to observe rotation-locked modulation effects on mesh frequency components.

2 Test Rig Configuration and Instrumentation for Coupled Spur Gear Dynamics

The experimental data were obtained from a two-stage spur gearbox comprising different teeth where the pinion drives 30 teeth, and 90 teeth drive the gear. Two PCB piezoelectric accelerometers were placed on the bearing casing at the input shaft and output shaft in the radial direction, as shown in Fig. 1. Through an experimental programme, a constant rotational speed of 130 rpm and an applied torque of 0.12 Nm were selected as reference control parameters. Effects of spur gear eccentricity were examined via lateral and torsional vibration responses, together with time evolving frequency content, using a LabVIEW based measurement environment. Data were acquired through an NI Compact-DAQ system (NI 9215), allowing subsequent digital signal processing and repeated testing for extraction of raw vibration characteristics. A sampling rate of 3100 (S/s) and a 20000-frequency sample were taken into consideration for the vibration measurement.

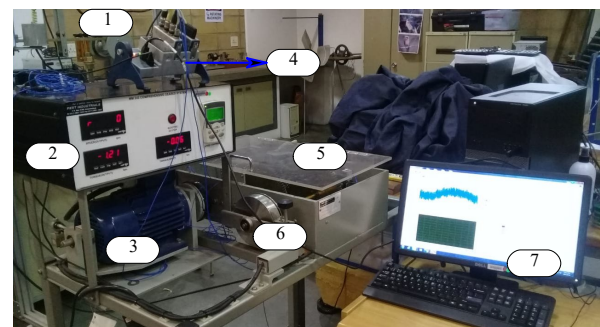


Fig.1 Test rig of comprehensive geared gearbox system 1-NI Compact DAQ Module,2-Input indicator system,3-Electric motor,4-accelerometers sensor, 5-Gear set, 6-Mechanical Brake dynamometer,7-computer.

Fig. 1 presents the experimental setup of a geared gearbox system used to investigate eccentricity effects on vibration response in a two-stage spur gear configuration. The setup includes three bearing supported shafts fixed to a steel frame, two stationary gears, and two shiftable gear sets. An interchangeable inertia disc is mounted on the second shaft, and the motor provides excitation through the transmission shaft. Mechanical coupling links the drive and input shafts, while the output shaft interfaces with a magnetic powder clutch brake. Operation of the gearbox is configured to be smooth and quiet, with relatively low vibration amplitudes. Eccentricity refers to the radial deviation of a pinion's or gear's rotational centre from its geometric centre. Gear eccentricity is one of the most common gear system defects affecting nonlinear response and mesh stiffness. In this case, the gear eccentricity fault is used to excite the system with the different eccentric masses to perceive the vibration behaviour of the geared system.

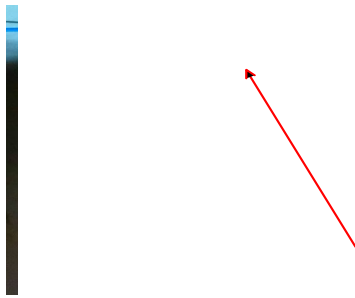


Fig.2 Localized Gear Eccentricity Identified Through Physical Inspection of the Test Rig

A compact two stage gearbox with a small installation footprint was employed, allowing straightforward placement even in constrained laboratory spaces. High quality construction materials were selected so that the system could tolerate heavy duty operating conditions without structural degradation. Power transmission from the input shaft to the output shaft is achieved through two spur gear stages, each designed to combine high mechanical efficiency with low backlash. The gearbox forms part of a three phase MM 242 Comprehensive Geared System, developed to operate on a 220 V power supply. Within this system, eccentricity faults were deliberately induced to excite the gear dynamics, as illustrated in Fig. 2. The excitation was achieved by mounting eccentric masses of 200 g, 400 g, and 890 g on the driven gear wheel. Each mass was positioned at a radial distance of 4 cm from the shaft axis and offset by 1.8 cm from the pitch circle, thereby introducing a controlled eccentricity error into an otherwise healthy spur gear system.

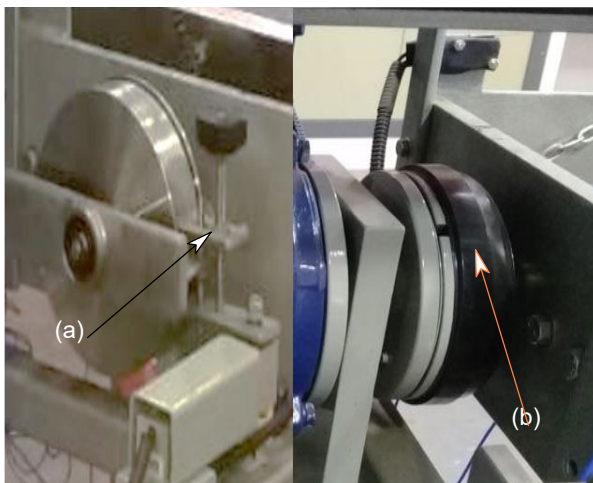


Fig.3 Dynamometer Configuration for (a) Braking Load Application and (b) Motor Drive Operation

A dynamometer is a device used to measure a spur gear's torque and rotational speed. Using a dynamometer in testing spur gears is to determine the gear's performance, efficiency, and durability under load and identify any defects or weaknesses. The data collected from the dynamometer helps analyse the gear's design and material, and allows for improvements to increase its

reliability and longevity. Fig. 3 shows the dynamometer of the motor and brake. Measurement of the gear system output power is achieved by coupling a mechanical brake dynamometer to the third, or output, shaft. Speed regulation of the machine is provided through an inverter, ensuring controlled operating conditions. Upstream in the drivetrain, an electronic clutch is used to connect the dynamometer motor to the first shaft, completing the power transmission path.

3 Data Measurement and Acquisition

Data measurement aims to define the variables of interest and choose appropriate methods for obtaining data, while data acquisition involves collecting the data. These steps are important because the quality of the data collected directly impacts the validity and reliability of research findings. Accurate data measurement and acquisition ensure that the data collected is relevant, representative of the population under study, and can be used to answer research questions and support conclusions. Fig. 4 below presents the data acquisition system architecture for vibration analysis.

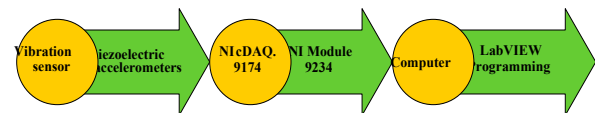


Fig.4 Schematic Representation of Data Acquisition System

National Instruments Compact-DAQ (Data Acquisition) modules are used in various applications to collect and process data from sensors and other devices for vibration analysis. As shown in Fig. 5, the data acquisition modules are connected to Compact-DAQ units to enable reliable data capture and validation. Synchronisation of measurements across the network is achieved through this configuration, with signal digitisation performed near the sensor location. Reduced electrical noise and less complex cabling result from this approach.

The measurement module was connected in a floating differential mode. For vibration monitoring, accelerometers with an acceleration sensitivity of 10.2 mV/(m/s²) were radially mounted on the bearing casing. Vibration signals were collected directly from the bearing housing via National Instruments data acquisition equipment. Such a setup enabled separate measurement of vertical vibration responses at both the input and output shafts of the gearbox.

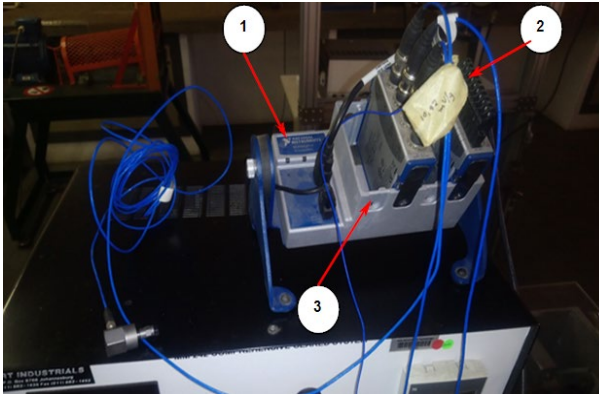


Fig.5 NI Compact DAQ Module: 1- Terminal block, 2- Sensors set, 3-Data Acquisition set

The NI 9215 is a four-channel signal acquisition module with a 16-bit resolution. The analogue inputs have a ± 10 V measurement range. The four channels can capture up to 100 kS/s per channel.

4 Vibration Signal processing

From a vibration perspective, a spur gear already generates a dominant periodic excitation at the gear mesh frequency. Eccentricity does not introduce a new dominant frequency. It modulates an existing one. Such modulation is deterministic, rotationally locked, and therefore well suited to frequency-domain analysis. FFT becomes effective because periodic modulation in time translates into structured sidebands in the frequency spectrum. The measured vibration signal be $x(t)$, acquired from an accelerometer mounted on the gearbox housing. For a single gear mesh harmonic, the vibration can be modelled as an amplitude-modulated sinusoid.

$$x(t) = A \cos(2\pi f_m t) + \frac{Am}{2} \cos[2\pi(f_m + f_r)t] \quad (1)$$

$$\Phi = \frac{Am}{2} \cos[2\pi(f_m - f_r)t] + \eta(t) \quad (2)$$

$$f_m = Zf_r = \frac{Z \cdot RPM}{60} \quad (3)$$

A is the nominal mesh vibration amplitude, f_m is the gear mesh frequency, f_r is the shaft rotational frequency of the eccentric gear, m is the modulation depth linked to eccentricity severity, ϕ is a phase constant, $\eta(t)$ represents noise and other vibration sources. The physical meaning becomes visible. Eccentricity causes symmetric frequency components around the gear mesh frequency, spaced by the shaft rotational frequency. Higher-order modulation terms produce additional sidebands at $f_m \pm kf_r$, where $k=1,2,3,\dots$. The vibration signal is sampled at frequency f_s , producing a discrete sequence $x[n]$, with $n = 0,1,\dots,N-1$. The Discrete Fourier Transform is defined as [19].

$$x[k] = \sum_{n=0}^{N-1} x[n] \omega[n] e^{-j2\pi kn/N} \quad (4)$$

where $\omega[n]$ is a window function applied to reduce spectral leakage, k is the frequency-bin index. A

mathematical de-noise filter for vibration can be written in a few standard forms. Choice depends on what the mechanical system is doing, because the filter should respect the physics, not only the spectrum. Start from a sampled vibration signal $y[n]$ with sampling rate F_s (Hz). A causal IIR filter can be expressed as:

$$x[n] = \sum_{k=0}^M b_k y[n-k] - \sum_{k=1}^N a_k x[n-k] \quad (5)$$

Design idea: choose a band $[f_1, f_2]$ that captures the mesh frequency and sideband neighborhood, then implement a Butterworth band-pass (flat passband, monotonic magnitude). Butterworth magnitude prototype for a low-pass has the well-known form

$$|H(j\omega)|^2 = \frac{G_0^2}{1 + \left(\frac{\omega}{\omega_c}\right)^{2n}} \quad (6)$$

Zero-phase filtering avoids phase distortion in time waveforms by applying forward and reverse filtering (often called forward-backward filtering). Many gear diagnostics prefer that, because phase shifts can blur impulsive features in the time domain.

In many experimental rigs and industrial machines, operating conditions are not perfectly stationary. Speed drifts, load varies, engagement stiffness evolves, sometimes subtly. Under such conditions, FFT alone compresses the entire signal history into one spectrum, averaging out temporal evolution. STFT is introduced not to change the physics, but to preserve time. It allows to observe how the spectral signature of eccentricity develops, shifts, or strengthens as the gear rotates or operating conditions evolve. Eccentricity, being synchronous with shaft rotation, remains visible in STFT as persistent, time-coherent sidebands around the gear mesh frequency. The Short-Time Fourier Transform of a continuous signal $x(t)$ is defined as

$$STFT_x(t, \omega) = \int_{-\infty}^{\infty} x(\tau) g(\tau - t) e^{-j\omega\tau} d\tau \quad (7)$$

where $g(\tau-t)$ is a window function centered at time and $\omega=2\pi f$ is angular frequency. When eccentricity induces continuous, rotation-locked modulation, the STFT representation reveals long-lasting, evenly spaced sidebands that track the gear mesh frequency over time. The method becomes particularly valuable under non-constant speed conditions, where FFT-based sidebands tend to appear smeared or significantly attenuated.

5 Waveform Response of the Gear System

A healthy gear was used as a baseline with zero loads applied with the purpose of conducting experiments at a normal or perfect spur gear system is to obtain a fundamental basis of the operational gearbox condition to provide meaningful outcomes. The vibration signal was collected in both the time- and frequency domains to visualize the results. During experiment testing, the de-noising technique was carried out for both healthy and faulty cases due to uncontrolled factors and background noise. The reference signal used to de-noise

noise from a defective gear is the vibration signal from a healthy gear. In this section, the signal with noise is decomposed and denoised by the level 3 threshold Haar wavelet transform method. Wavelet transform was employed to reveal features of data that noise might mask and provides a sparse representation of the signal to quantify the signal analysis.

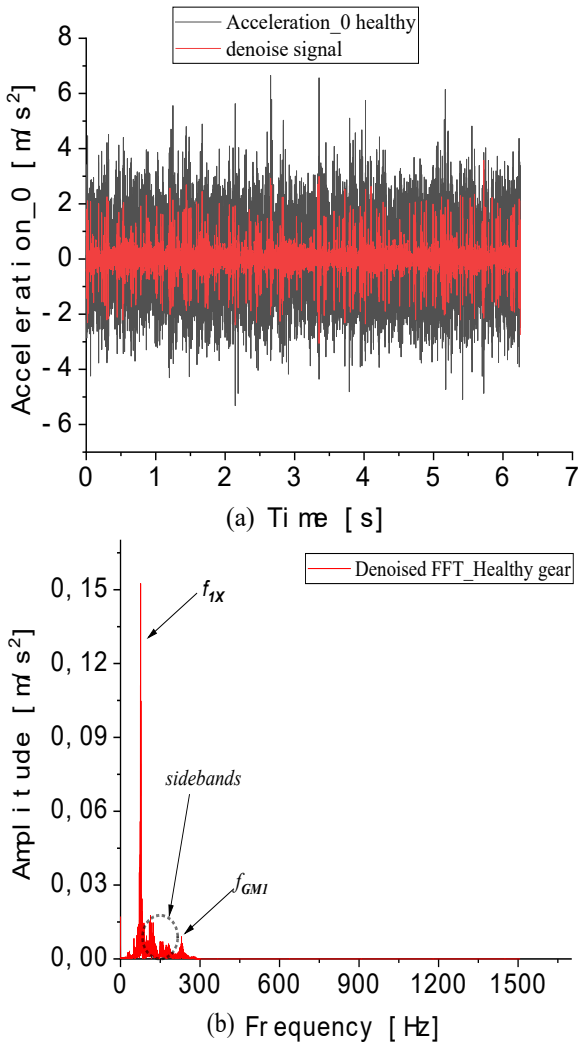


Fig.6 (a) Time-Domain vibration signal results in perfect state of mixture signal of original and de-noised, (b) Frequency-Domain vibration signal in perfect state

The time domain clearly demonstrates how the vibration evolved over the time. They might seem to be incredibly complex graphs, but they frequently can detect errors that other methods cannot do. Fig. 6(a) illustrates how de-noising an experimental Time-Domain vibration signal results in healthy gear. Depicts the mixture of original and de-noise signals to show how the original signal is de-noised. After filtering some noise, peaks become visible. The final de-noised signal shows that the gear transmission was proper and at the maximum amplitude of 2.4 m/s^2 . However, to simplify the analysis of the system's vibration behaviour, a spectrum of the same results as in the time domain was created and is shown in Fig. 6(b). The Fast Fourier Transform (FFT) is a development of the DFT, which eliminates redundant terms from the mathematical algorithm to minimize the

number of operations required. As a result, samples can often be used without slowing down the transformation in the spectrum. Therefore, the frequency of the input rotational speeds shaft (f_{IX}) occurs at 76 Hz with an acceleration amplitude of 0.15 m/s^2 , the first tooth mesh (f_{GM1}) occurs at 230.4 Hz at a very low amplitude of 0.009 m/s^2 . Observation of the vibration behaviour of a healthy gear shows that the system is running based on the vibration response. Regardless of the minor sideband bands appearing on the FFT results that might be agitated by small variable factors during the experiment, even though we tried to filter some noise, it was not easy to control what was happening around the gears. Nevertheless, those characteristics indicate that the gearbox is still under normal circumstances.

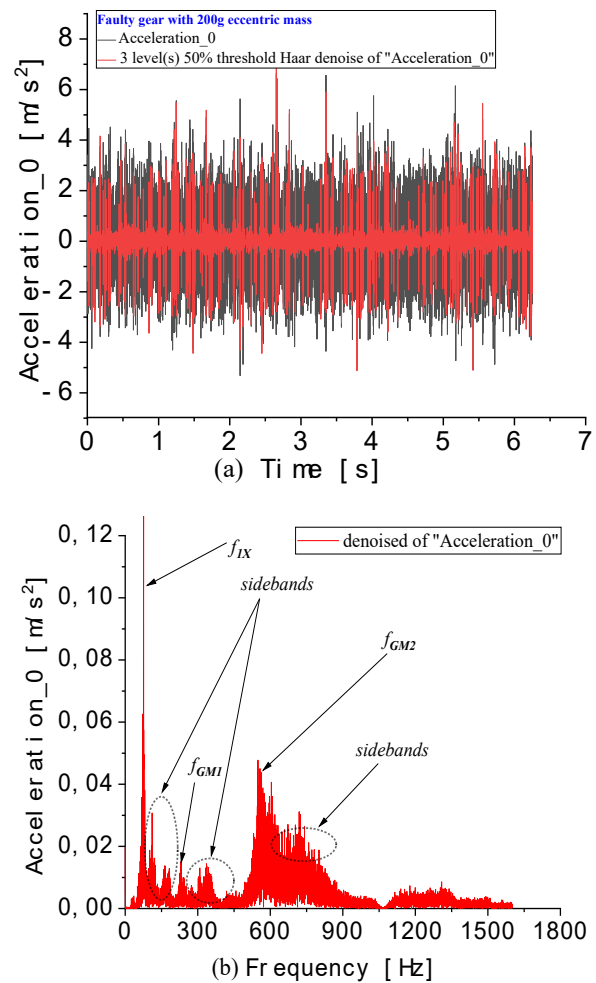


Fig.7 (a) Time-Domain vibration signal results with eccentricity fault @200g eccentric mass of mixture signal of original and de-noised; (b) Frequency-Domain vibration signal results with 200g eccentric mass

Usually, these types of patterns can be best understood by interpreting the spectrum, not the waveform, due to the nonlinear factors. Regarding system nonlinearity, gear eccentricity is regarded as major system nonlinearity in this work. In addition, the eccentricity of the gear wheel contributes significantly to the vibration of the gearbox system in the radial direction. In analysing the time domain, only the variation in amplitude was taken into account because of non-

linearity. Compared to the healthy gear, the faulty gear with 200g slightly increases by 4.8 m/s^2 in vibration amplitude at 2.6 seconds Fig. 7(a). As shown in Fig. 7(b), the synchronous speed of the input shaft (f_{IX}) at 76 Hz decreased from 0.15 to 0.12 vibration amplitude. It also noticed that at 230.4 Hz, gear mesh frequency (f_{GM1}) was slightly incremented by 0.005 amplitude from the healthy gear vibration. Because of the eccentric mass, the sidebands of the 1st gear mesh started to increase a bit, and the frequencies component of the 2nd (f_{GM2}) gear mesh harmonics seems to start developing along with its sidebands at 550 Hz.

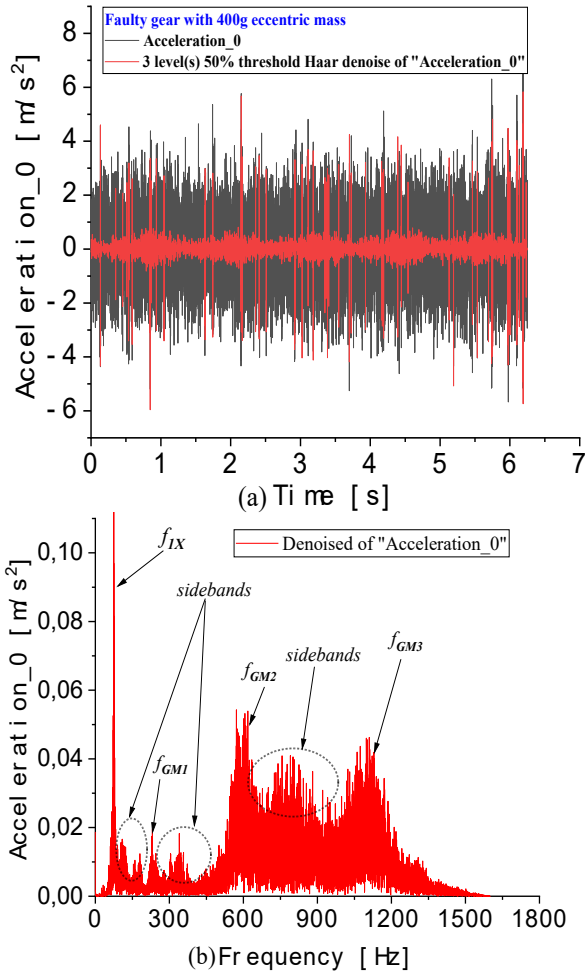


Fig.8 (a) Time-Domain vibration signal results with eccentricity fault @400g eccentric mass of mixture signal of original and de-noised; (b) Frequency-Domain vibration signal results with 400g eccentric mass

In Fig. 7(a) it clearly noticed that in this case at 0,8, 2.1, and 3.1 seconds accordingly. At the same time, meshing is generated. It rises when force is more significant and gets the higher amplitude of vibration, and when gears further apart get the lower amplitude of vibration at passes 1.4, 2.6, and 3.6 seconds when force is weaker. In addition, this system vibrates due to the dynamic forces caused by the gear mesh and eccentricity. According to observations of this system's dynamic force characteristics in the time domain, eccentricity, in this case, causes the increment of vibration amplitude to rise in comparison to both a healthy gear and a defective

gear with a 200g eccentric mass case. The GMF harmonics and their sidebands were also plotted using the FFTs to analyse the dynamic force characteristic frequencies. The FFT test rig's vibration characteristics with a 400g eccentric mass are shown in Fig. 7(b). The highest rotation speed shaft oscillation (f_{IX}) as 76 Hz, and the maximum amplitude was noted to be 0.11 m/s^2 . The first GMF (f_{GM1}) is detected at 230,4 Hz and has an amplitude of $0,017 \text{ m/s}^2$. On the right side, its sidebands rapidly rose to $0,018 \text{ m/s}^2$ amplitude at 340,32 Hz, whereas on the left, sidebands only marginally increased to $0,012 \text{ m/s}^2$ at the low frequency of 180,64 Hz. At 606 Hz frequency of the 2nd gear mesh (f_{GM2}) was observed with a higher amplitude of $0,032 \text{ m/s}^2$ than the first, than the amplitude value of 1st gear mesh, its sidebands developed between 617-650 Hz with the amplitude of $0,05 \text{ m/s}^2$. Moreover, in this case, more modulation resulted from the variation of the forces generated by gear meshing due to eccentricity fault under 400g eccentric mass case. However, 1128.64 Hz has been identified as the 3rd gear mesh frequency (f_{GM3}) with an amplitude of $0,04 \text{ m/s}^2$.

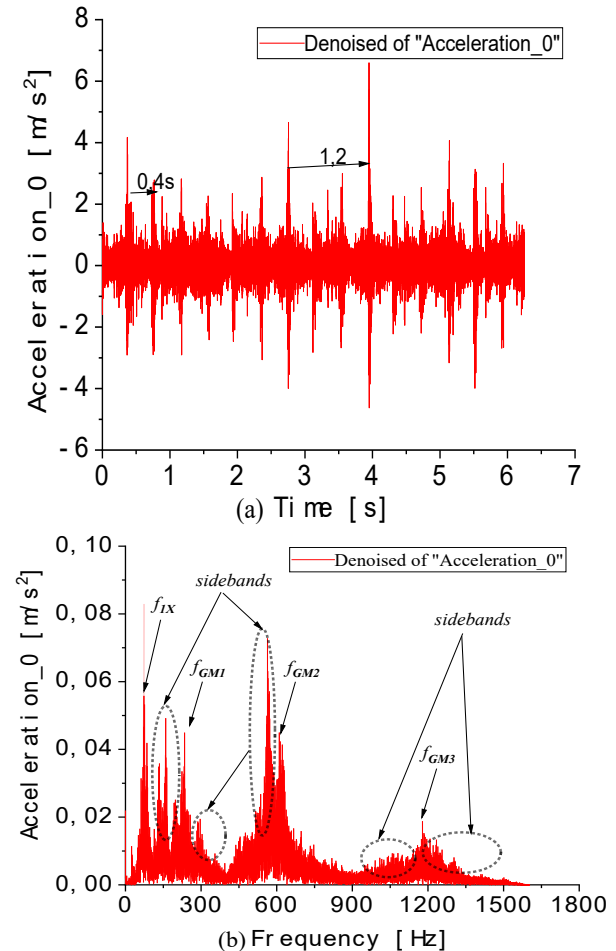


Fig.9 (a) Time-Domain vibration signal results with eccentricity fault @890g eccentric mass of de-noised; (b) Frequency-Domain vibration signal results with 890g eccentric mass

Gear teeth with abrupt changes in stiffness, rough surfaces, and increased transmission error caused by gear eccentricity are the main factors that induce vibration impulses. As depicted in Fig. 9(a), the

eccentricity impacts the gear transmission system, particularly at high ratios. Gear mesh signatures typically include sidebands that identify other vibrations that are present, and they are a result of modulation. Strong gear mesh frequency acts as a carrier frequency for the present vibration. Sidebands are, therefore, a visual representation of low-level vibrations transmitted by strong vibrations. Analysing amplitude modulations (sidebands) along the gear mesh frequency can be quite useful in detecting gear deterioration. Furthermore, since the gear meshing vibrations and their harmonics carry most of the gear fault information and their sidebands, denoising the spectrum signal will still preserve that information. Sidebands rise due to non-linearity in the system and also help detect the fault. To notice the fault symptoms, sidebands around the GMF developed by the carrier frequency are discovered in the Fourier spectrum shown in Fig. 9(b). It was also noticed that the input speed shaft resonant frequency was intensely decreased from 0.11 m/s^2 to 0.055 m/s^2 amplitude, and it is sub-harmonic at 24.34 Hz was formed with the amplitude of 0.011 m/s^2 . The one-times GMF (fGM1) at 230.4 Hz was spotted with an increased amplitude by 0.028 m/s^2 from the fault case with 400g eccentric mass. Its sidebands from the left side rise to 0.024 m/s^2 , while on the right side, they have an amplitude of 0.018 m/s^2 . It has been noticed that the amplitude of the 2nd GMF (fGM2) at 606 Hz is equal to that of the 1st GMF (fGM1), which is 0.045 m/s^2 at this stage. Its amplitude modulations on the right-side increase massively to the amplitude of 0.73 m/s^2 at 562.24 Hz frequency, where it can be seen that its sidebands are greater than the 1st and 2nd carrier frequency. Left side sidebands of (fGM2) also rise to the 0.41 m/s^2 amplitude at 620.96 Hz , which is also greater than the amplitude of carrier frequency (fGM2). The 3rd GMF (fGM3) amplitude increased to 0.019 m/s^2 at the super harmonic area with a frequency of 1175 Hz .

6 Short-Time Fourier Transform

The STFT is used to recover the features not captured in FFT and spectral leakage during the denoising process. The STFT divides a signal into discrete time windows to determine the frequency content within each window. However, the STFT technique converts a 1D time signal to a 2D time scale to detect changes in frequency over a short period. The STFT localization overcomes the limitations of fixed window size, which previously limited fault diagnosis. Furthermore, STFT is helpful in analysing varying non-stationary signals, making it an ideal tool for time-frequency analysis. In this section, STFT analysis was employed as a time-frequency technique.

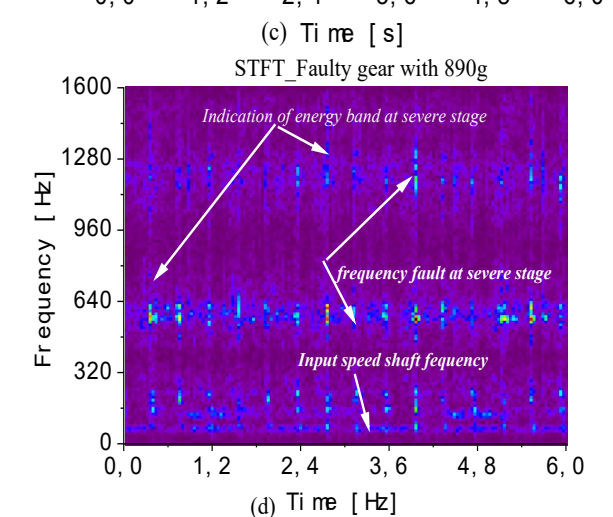
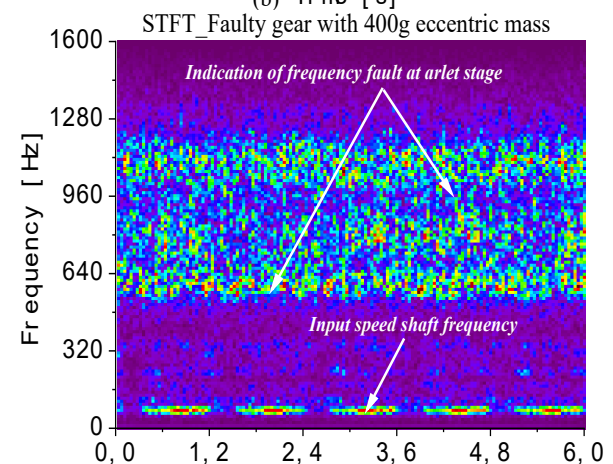
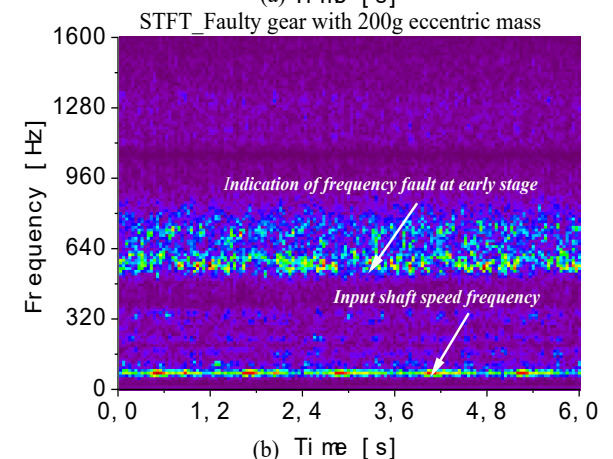
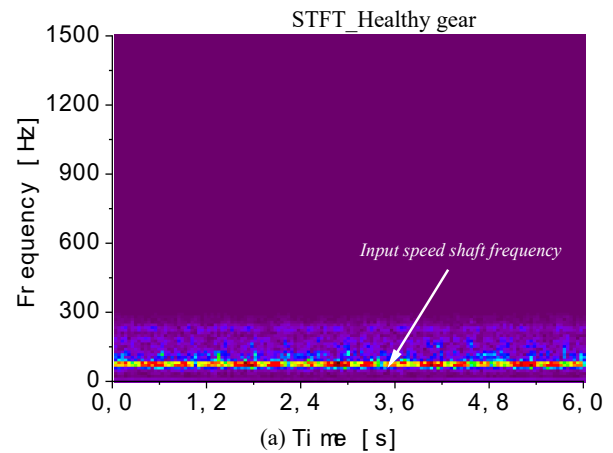


Fig.10 (a) Time-Domain vibration signal results with eccentricity fault @890g eccentric mass of de-noised; (b) Frequency-Domain vibration signal results with 890g eccentric mass

Fig. 10 presents the time–frequency representation obtained from the Short Time Fourier Transform, illustrating the temporal evolution of frequency components associated with nonlinear and non-stationary vibration signals. The spectrum in Fig. 10(a) indicates a dominant frequency component of approximately 80 Hz over a duration of about 6 s, while frequency fluctuations extend to nearly 280 Hz. Energy concentration is primarily observed within the low-frequency band, which is characteristic of the healthy gear condition. Such behaviour reflects a stable dynamic response, although a rise in vibration amplitude is evident at the input shaft rotational frequency. A contrasting behaviour is observed in Fig. 10(b), where frequency fluctuations become more pronounced within the approximate range of 485 Hz to 800 Hz. Such elevated and dispersed spectral content suggests the presence of transmission errors induced by gear eccentricity. The redistribution of energy toward higher frequency bands indicates altered meshing dynamics and enhanced modulation effects, consistent with eccentricity-related excitation within the gearing system. Fig.10(c) shows strongly raised frequency oscillations from 485 Hz to 1280 Hz. By looking at the results, it detected that, in this case, the fault is a moderate stage. Fig. 10(d) shows the faded frequency band at 85 Hz to 1440 Hz, resulting in the gear system's low energy band dispersion. Therefore, it indicates the high transmission error caused by a high ratio of gear eccentricity, noting that the severe fault that occurred means that it reached a dangerous stage where the machine cannot operate because it can also affect the other components in the gear system.

7 Conclusion

Gear eccentricity generates a vibration response that is intrinsically subtle, strongly coupled to rotational kinematics, and easily submerged within dominant meshing dynamics and measurement noise. Early and intermediate fault stages therefore remain difficult to resolve experimentally, not due to lack of analytical tools, but because the physical manifestation of eccentricity is low-energy and modulation-driven. Many contemporary diagnostic frameworks, particularly those based on complex signal decomposition or data-driven inference, demonstrate high sensitivity yet often detach detection outcomes from the underlying mechanics of fault development. Emphasis on physically interpretable frequency-domain and time-frequency representations offers a necessary counterbalance, allowing modulation mechanisms linked to eccentricity to be traced explicitly to gear rotation and meshing processes. Such an approach strengthens diagnostic transparency, supports fault severity interpretation, and improves confidence in experimental assessments, especially under non-ideal operating conditions where speed variation and noise cannot be avoided.

References

1. Huo, G., Iglesias-Santamaria, M., Zhang, X., Sanchez-Espiga, J., Caso-Fernandez, E., Jiao, Y. and Viadero-Rueda, F., 2024. Influence of eccentricity error on the orbit of a two-stage double-helical compound planetary gear train with different mesh phasing configurations. *Mechanism and Machine Theory*, 196, p.105634.
2. Chen, Z., Ning, J., Wang, K. and Zhai, W., 2021. An improved dynamic model of spur gear transmission considering coupling effect between gear neighboring teeth. *Nonlinear Dynamics*, 106(1), pp.339-357.
3. Yang, L., Zeng, Q., Yang, H., Wang, L., Long, G., Ding, X. and Shao, Y., 2022. Dynamic characteristic analysis of spur gear system considering tooth contact state caused by shaft misalignment. *Nonlinear Dynamics*, 109(3), pp.1591-1615.
4. Shi, J.F., Gou, X.F. and Zhu, L.Y., 2021. Generation mechanism and evolution of five-state meshing behavior of a spur gear system considering gear-tooth time-varying contact characteristics. *Nonlinear Dynamics*, 106(3), pp.2035-2060.
5. Abdallah, O. and Sassi, S., 2024. Contribution of friction-induced vibration to the realistic failure analysis of spur gear cracked teeth. *Engineering Failure Analysis*, 158, p.107956.
6. Zhou, W., Zhu, R., Li, Z., Liu, W. and Wang, J., 2024. An improved dynamic model of spur gears considering delayed meshing out of the contact point due to root crack. *Mechanical Systems and Signal Processing*, 212, p.111325.
7. Shi, H., Chen, W., Li, J., Wang, Z. and Jiang, L., 2024. Vibration stability and bifurcation analysis of spur gear systems based on time-varying backlash and random load. *International Journal of Non-Linear Mechanics*, 160, p.104648.
8. Ali, Y., Tlija, M., Shah, S.W., Arif, A. and Siddiqi, M.R., 2025. Intelligent condition monitoring of gear system at variable load and variable speed using vibration data. *Advances in Mechanical Engineering*, 17(9), p.16878132251364692.
9. Sharma, V., Parey, A., Singh, A.P., Paul, A. and Singh, Y., 2021. Detection of Fault in a Bevel Gearbox Under Varying Speed Conditions. In *Recent Advances in Mechanical Engineering: Select Proceedings of ICRAME 2020* (pp. 697-709). Singapore: Springer Singapore.
10. Rai, A., Kapu, V.P., Balaji, P.S. and Tiwari, P., 2024. Gear fault diagnosis based on complex network theory and error-correcting output codes: Multi class support vector machine. *Proceedings of the Institution of Mechanical Engineers, Part I: Journal of Systems and Control Engineering*, 238(6), pp.1135-1152.
11. An, X., Pan, L., Li, W. and Xiao, W., 2025, August. Gear fault diagnosis via demodulation analysis based on NA-MEMD. In *Journal of Physics:*

- Conference Series (Vol. 3079, No. 1, p. 012073). IOP Publishing.
12. Mansi, Saini, K., Vanraj and Dhimi, S.S., 2021. MODWT and VMD based intelligent gearbox early stage fault detection approach. *Journal of Failure Analysis and Prevention*, 21(5), pp.1821-1837.
 13. Inyang, U.I., Petrunin, I. and Jennions, I., 2024. A composite learning approach for multiple fault diagnosis in gears. *Proceedings of the Institution of Mechanical Engineers, Part O: Journal of Risk and Reliability*, 238(1), pp.158-171.
 14. Bouzouidja, M., Soualhi, M., Soualhi, A. and Razik, H., 2024. Detection and diagnostics of bearing and gear fault under variable speed and load conditions using heterogeneous signals. *Energies*, 17(3), p.643.
 15. Kumar, S. and Kumar, R., 2021. Diagnosis of an incipient defect in a worm gearbox using minimum entropy deconvolution and local cepstrum. *Measurement Science and Technology*, 32(5), p.054002.
 16. Sigonde, V.C., Sozinando, D.F., Tchomeni, B.X. and Alugongo, A.A., 2025. Coupled Nonlinear Dynamic Modeling and Experimental Investigation of Gear Transmission Error for Enhanced Fault Diagnosis in Single-Stage Spur Gear Systems. *Dynamics*, 5(3), p.37.
 17. Salunkhe, V.G., Salodkar, Y.R., Mohite, A.S., Lad, H.P., Patil, S.R., Khot, S.M., Desavale, R.G. and Jagadeesha, T., 2025. Fault evolution characteristics analysis of spur gear based on dimensional technique and support vector machine. *Journal of Nondestructive Evaluation, Diagnostics and Prognostics of Engineering Systems*, 8(4), p.041006.
 18. Matania, O., Bechhoefer, E., Blunt, D., Wang, W. and Bortman, J., 2024. Anomaly Detection and Remaining Useful Life Estimation for the Health and Usage Monitoring Systems 2023 Data Challenge. *Sensors*, 24(13), p.4258.
 19. Sozinando, D.F., Tchomeni, B.X. and Alugongo, A.A., 2023. Experimental study of coupled torsional and lateral vibration of vertical rotor-to-stator contact in an inviscid fluid. *Mathematical and Computational Applications*, 28(2), p.44.